AKARI INFRARED CAMERA OBSERVATIONS OF THE 3.3 μm PAH FEATURE IN Swift/BAT AGNs

Angel Castro[1], Takamitsu Miyaji[1,2], Mai Shirahata[3,4], Kohei Ichikawa[5], Shinki Oyabu[6], David Clark[1], Masatoshi Imanishi[7], Takao Nakagawa[4], and Yoshihiro Ueda[5]

[1]Instituto de Astronomía, Universidad NacionalAutónoma de México (UNAM), Ensenada, Baja California, México
[2]University of California, San Diego, Center for Astrophysics and Space Sciences, La Jolla, CA 92093-0424, USA
[3]National Astronomical Observatory of Japan (NAOJ), 2-21-1 Osawa, Mitaka, Tokyo 181-8588, Japan
[4]Institute of Space and Astronautical Science (ISAS), 3-1-1 Yoshino-dai, Chuo-ku, Sagamihara 252-5210
[5]Department of Astronomy, Kyoto University, Kitashirakawa-Oiwake-cho, Sakyo-ku, Kyoto 606-8502
[6]Graduate School of Science, Nagoya University, Furo-cho, Chikusa-ku, Nagoya, Aichi 464-8602, Japan
[7]Subaru Telescope, 650 North A'ohoku Place, Hilo, Hawaii, 96720, USA

E-mail: acastro@astrosen.unam.mx

ABSTRACT

Using the InfraRed Camera (IRC) on board the infrared astronomical satellite AKARI we study the 3.3 μm polycyclic aromatic hydrocarbon (PAH) feature and its connection to active galactic nucleus (AGN) properties for a sample of 54 hard X-ray selected bright AGN, including both Seyfert 1 and Seyfert 2 type objects. The sample is selected from the 9-month Swift/BAT survey in the 14–195 keV band and all of the sources have known neutral hydrogen column densities (N_H). The 3.3 μm PAH luminosity ($L_{3.3\mu\mathrm{m}}$) is used as a proxy for star-formation (SF) activity and hard X-ray luminosity ($L_{14-195\mathrm{keV}}$) as an indicator of the AGN power. We explore for possible difference of SF activity between type 1 (un-absorbed) and type 2 (absorbed) AGN. We use several statistical analyses taking the upper-limits of the PAH lines into account utilizing survival analysis methods. The results of our $\log(L_{14-195\mathrm{keV}})$ versus $\log(L_{3.3\mu\mathrm{m}})$ regression shows a positive correlation and the slope for the type 1/unobscured AGN is steeper than that of type 2/obscured AGN at a 3σ level. Also our analysis shows that the circum-nuclear SF is more enhanced in type 2/absorbed AGN than type 1/un-absorbed AGN for low $L_{14-195\mathrm{keV}}$ luminosity/low Eddington ratio AGN, while there is no significant dependence of SF activity on the AGN type in the high $L_{14-195\mathrm{keV}}$ luminosities/Eddington ratios.

Key words: galaxies: active — galaxies: Seyfert — X-rays: galaxies.

1. DESCRIPTION OF THE RESEARCH

In this work, we investigate the 2.5–5 μm low-resolution (R∼120) spectra obtained with the InfraRed Camera (IRC) instrument on the Japanese space infrared observatory AKARI for a sample of 54 AGN with various levels of obscuration selected from the 9-month catalog (Tueller et al., 2008) of the Swift/BAT survey, which is sensitive to very high X-ray energies (14–195 keV). In our sample, 26 AGN are optical type 1 AGN (Seyfert optical type ≤ 1.5) and 28 type 2 AGN (Seyfert optical type > 1.5). Our selected sample also has detailed X-ray spectroscopy (0.3–12 keV) (Winter et al., 2009; Ichikawa et al., 2012). For all objects in our sample X-ray derived neutral hydrogen column densities were obtained mainly by analyzing spectra from the XMM-Newton, ASCA, Suzaku, and Swift/XRT. We use the 3.3 μm PAH emission detected in our spectral range as a proxy for the SF activity to explore the link between AGN activity, column densities towards the nucleus, AGN type and SF. Detailed results have been reported in Castro et al. (2014).

Table 1
Linear regression parameters obtained using the E-M method under ASURV.

Sample	No.	Up.[†]	a_0	b_0	$\langle\log(L_{3.3\mu m})\rangle$	P[‡]
$\log(L_{3.3\mu m}) = a_0\{\log(L_{14-195\mathrm{keV}}) - 43.64\} + b_0$:						
All AGN	54	30	0.42±0.14	40.20±0.11	40.07±0.12	0.01
Optical type 1	26	20	1.05±0.27	39.92±0.24	39.68±0.22	0.02
Optical type 2	28	10	0.11±0.17	40.27±0.12	40.23±0.11	0.66
$\log(L_{3.3\mu m}/M_{\mathrm{BH}}) = a_0\{\log(L_{14-195\mathrm{keV}}/M_{\mathrm{BH}}) - 35.42\} + b_0$:						
All AGN	54	30	0.73±0.17	31.97±0.13	31.88±0.13	0.002
Optical type 1	26	20	1.56±0.37	31.55±0.26	31.62±0.21	0.005
Optical type 2	28	10	0.62±0.23	32.16±0.16	32.01±0.16	0.10

Notes: [†] Number of upper-limits included, [‡] Correlation probability by Cox's proportional hazard model.

Table 2
Two sample tests for optically classified AGN.

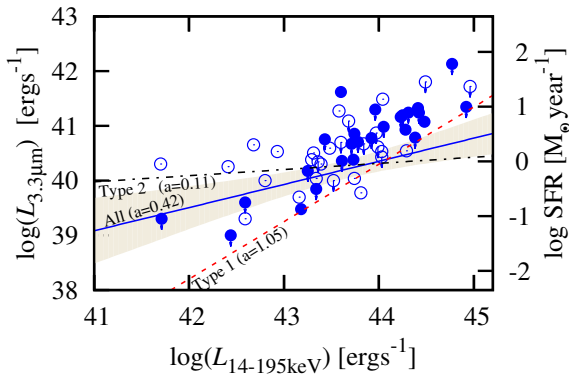| Criteria				$\langle\log(L_{3.3\mu m})\rangle$		Gehan's	logrank	Peto&Peto
	No.	n_{sy1}	n_{sy2}	Type 1	Type 2	Prob.	Prob.	Prob.
$\log(L_X) \leq 43.64$	26	9	17	39.44±0.28	40.19±0.13	0.04	0.02	0.02
$\log(L_X) > 43.64$	28	17	11	40.59±0.09	40.29±0.19	0.66	0.34	0.50
$\log(L_X/M_{\mathrm{BH}}) \leq 35.43$	25	10	15	31.17±0.15	31.66±0.13	0.14	0.09	0.12
$\log(L_X/M_{\mathrm{BH}}) > 35.43$	29	16	13	32.21±0.19	32.62±0.20	0.21	0.18	0.18

Figure 1. $\log(L_{14-195\mathrm{keV}})$ versus $\log(L_{3.3\mu m})$ relation. On the right vertical axis of panel is the approximate SFR is shown. Blue filled circles are for optical Seyfert 2 while blue open circles are for Seyfert 1 sources. Arrows are for upper-limits.

2. ANALYSIS AND RESULTS

To test the difference of SF activity between different types of AGN the several correlation analyses have been made. The regression has been made using the E-M algorithm (included in the ASURV package; Isobe et al. (1986)) to account for upper-limits of the $L_{3.3\mathrm{m}}$. If the minimum χ^2 (bestfit case) is smaller than 2.7 below the χ^2 value at $f_{3.3} = 0$, we consider the line detected and report the bestfit $f_{3.3}$. Otherwise, we consider it a non-detection.

We have compared the $\log(L_{3.3\mu m})$ versus $\log(L_{14-195\mathrm{keV}})$ (see Figure 1) and $\log(L_{3.3\mathrm{m}}/M_{\mathrm{BH}})$ versus $\log(L_{14-195\mathrm{keV}}/M_{\mathrm{BH}})$ correlations for optical type 1 and type 2 AGN (see Table 1). Strong correlation is found for both cases. We have sub-divided our sample into low- and high-luminosity subsamples (in reference to the mean $\log(L_{14-195\mathrm{keV}})$ value of the whole sample). In order to compare this two sub-populations (for both type 1 and type 2 sources; see Table 2) we have performed the two-sample test under ASURV revealing that for the low-luminosity $\log(L_{3.3\mu m})$-$\log(L_{14-195\mathrm{keV}})$ space the SFR is more enhanced in type 2/absorbed AGN than type 1/un-absorbed AGN. This finding was also verified using the Bootstrap method.

3. CONLUSIONS

Strong correlation is found between $\log(L_{14-195\mathrm{keV}})$ and $\log(L_{3.3\mu m})$ as well as between $\log(L_{14-195\mathrm{keV}}/M_{\mathrm{BH}})$ and $\log(L_{3.3\mu m}/M_{\mathrm{BH}})$ for both optical and X-ray classified type 1 AGN. We have found no statistical difference in the mean circum-nuclear star-formation rate (SFR), traced by the PAH 3.3 μm emission, between type 1 and type 2 AGN for our overall sample. Limiting the analysis to low $L_{14-195\mathrm{keV}}$ luminosity AGN, however, stronger nuclear starburst activity is found in type 2 AGN than in type 1 AGN. There is no significant difference in the SF activity betwen high $L_{14-195\mathrm{keV}}$ type

1 and type 2 AGN. A similar trend has been found for the specific SFR, between low and high Eddington ratio samples, although the statistical significance is lower. Our results suggest that the difference between type 1/type 2 in low $L_{14-195\mathrm{keV}}$ luminosity AGN may reflect an evolution sequence, where more obscuring material is available around low $L_{14-195\mathrm{keV}}$ luminosity type 2 AGN when the circum-nuclear SF is feeding the central engine. At high $L_{14-195\mathrm{keV}}$, the difference between the two types may be mainly from the orientation effect.

ACKNOWLEDGMENTS

REFERENCES

Castro, A., Miyaji, T., Shirahata, M., Ichikawa, K., Oyabu, S., Clark, D., Imanishi, M., Nakagawa, T. & Ueda. Y., 2014, AKARI InfraRed Camera Observations of the 3.3 μm PAH feature in Swift/BAT AGNs, (PASJ in press:arxiv.org/abs/1408.3172)

Ichikawa, K., Ueda, Y., Terashima, Y., Oyabu, S. & Gandhi, P., 2012, Mid- and Far-Infrared properties of a complete sample of local AGNs, ApJ, 754,45

Imanishi, M., Nakagawa, T., Shirahata, M., Ohyama, Y. & Onaka, T., 2010, AKARI/IRC infrared 2.5-5μm spectroscopy of a large sample of LIRGs, ApJ, 681, 113

Isobe, T., Feigelson, E. D. & Nelson, P. I., 1986, Statistical methods for astronomical data with upper limits. II. Correlation and regression, ApJ, 306, 490-507

Tueller, J., Mushotsky, R., Barthelmy, S., Cannizzo, et al., 2008, The 9-month Swift-BAT All-Sky Hard X-ray Survey, ApJ, 681, 113

Winter, L.M., Mushotzky R., Reynolds, C. & Tueller, J., 2009, X-ray spectral properties of the BAT AGN sample, ApJ, 690, 1322